Derivation of Radiation from a Dipole immersed in a Homogeneous Magnetized Plasma

Laura Florescu
New York University

August 20, 2022

Abstract

We are considering a dipole antenna immersed in cold plasma and investigate its radiation patterns. We are solving Maxwell's equations using (1) analytic solutions for the case when the antenna is parallel to the magnetic field B_0 and (2) numerical solutions for any orientation and angle θ of the antenna.

We investigate various phase velocities regimes as well as the effect of varying the frequency and the plasma parameters on the electromagnetic waves are presented and discussed.

1 Introduction

In the 60's there seemed to be considerable interest ([WB69], [WB72], [WB692], [SHM]) exploring VLF radiation originating from dipoles in cold, anisotropic, homoegenous magnetized plasma. An anisotropic medium is important in the fabrication of modern radio electronics and in astrophysics and plasma physics applications among others. Furthermore, considering radiation from sources in a cold, uniform magnetized plasma can provide insight into the problem of focusing of radiation [SHM].

An especially interesting source to consider is a dipole antenna, as in plasma, it can launch EM waves in addition to electrostatic waves. Moreover, the far field behavior of dipole antenna can be changed by adjusting both the operating frequency and the applied magnetic field. Since no physical antenna radiates uniformly in all directions and it radiates EM waves better in certain directions than others, there is a need to understand radiation patterns. They possess a practical worth in providing insight into the coupling between VLF antenna systems and the magnetospheric plasma, as their details are especially important if the satellite transmitter is a low-power device, since the possibility of generating waves of useful amplitude may depend on maximizing the flow of power at a given wave normal distribution [WB72], [WB692]. The consideration of VLF emissions obtained using a transmitter aboard a magnetospheric satellite could provide information about optimizing the production of longitudinally propagating waves and increasing the output power of the satellite transmitter, thus of significant importance in the design of a VLF satellite transmitting system [WB69].

This study finds a variety of other applications, one outstanding one being a diagnosis of the plasma without disturbing it [SHM]. Conventional diagnostic devices such as probes for measuring electrostatic and magnetic fields not only contaminate the plasma but are too large for the investigation of the microscopic structure of the plasma. Thus this analysis would have two important scopes: a characterization of plasma and an exploration of antenna design, as efficiency would be quantified by the EM wave scattering by the plasma wave under investigation.

Due to the complexity of parameter tensors in the dielectric tensor, solving Maxwell equations for an anisotropic magnetized plasma and deducing the radiation patterns for an electric dipole require involved analytical calculations. The papers cited above employed a variety of techniques such as saddle point integrations, Green function, full wave coordinates.

The present paper considers a modern twist to the same type of problems, focusing on the radiation patterns arising from each of the spherical coordinates of the electromagnetic fields. We present our problem in Section 2. We obtain the fundamental solutions of a system of Maxwell's equations for a cold, anisotropic, homogeneous magnetoplasma in Section 3.1. In particular, we apply these to a small antenna dipole in Section 3.2, and we consider the radiation patterns in Section 4. We then present several electromagnetic radiation patterns plots. Next, in Section 5, we investigate these with respect to various phase velocities, dipole lengths, frequencies and far-field radii at which the patterns are considered. We find interesting correlations of the lobe predominance to the increasing phase velocities and radii, as well as rotational symmetries.

2 Formulation

2.1 Dielectric tensor and dispersion relations

We solve Maxwell's equations for **E** and **H** outside of a dipole antenna in a magnetized plasma. For these derivations, we assume that the plasma is homogeneous and characterized by a dielectric tensor

$$K = \begin{pmatrix} K_\perp & -K_\times & 0 \\ K_\times & K_\perp & 0 \\ 0 & 0 & K_\parallel \end{pmatrix} \quad (1)$$

The basic equations we are going to investigate are

$$\begin{aligned} \nabla \times E &= i\omega\mu_0 H \\ \nabla \times H &= -i\omega\epsilon_0 K E \end{aligned} \quad (2)$$

The relationship between the components of K and ω is given by:

$$\begin{aligned} K_\perp &= 1 - \frac{\omega_{pe}^2}{\omega^2 - \omega_{ce}^2} \\ K_\times &= i\frac{\omega_{pe}^2 \frac{\omega_{ce}}{\omega}}{\omega^2 - \omega_{ce}^2} \\ K_\parallel &= 1 - \frac{\omega_{pe}^2}{\omega^2}, \end{aligned}$$

where $\frac{\omega_{pe}}{\omega_{ce}} = a$, $\frac{\omega}{\omega_{ce}} = b$, $k_0 = \frac{\omega}{c}$ and the ω_{ce}, ω_{pe} are the usual plasma frequencies.

Using these ratios, we can write the components in the following way:

$$\begin{aligned} K_\perp &= 1 - \frac{a^2}{b^2 - 1} + \epsilon i \\ K_x &= i\frac{a^2}{(b^2-1)b} \\ K_\parallel &= 1 - \frac{a^2}{b^2} + \epsilon i \end{aligned} \quad (3)$$

We add the complex parts to avoid singularities in the real plane, which should result in smoother the radiation patterns, and we vary the ratios of the plasma frequencies to explore various phase velocities. Thus, we shall consider the ratios $\frac{a}{b}$ as the varying phase velocities which will allow us to explore the characteristics of radiation patterns. The reason varying phase velocities gives insight is that they correspond to various wave regimes as considered in [ABB].

We will have the following expression for the dielectric tensor:

$$K = \begin{pmatrix} K_\perp - k_z^2\cos^2\theta & -K_\times & k_z^2\cos\theta\sin\theta \\ K_\times & K_\perp - k_z^2 & 0 \\ k_z^2\cos\theta\sin\theta & 0 & K_\parallel - k_z^2\sin\theta \end{pmatrix} \quad (4)$$

3 Derivations

3.1 Analytic solutions for antenna parallel to B_0

We start with Maxwell's equations in cylindrical geometry, in Fourier domain:

$$\begin{aligned} -ik_z E_\theta &= -i\omega B_r \\ ik_z E_r - \frac{\partial E_z}{\partial r} &= -i\omega B_\theta \\ \frac{1}{r}\frac{\partial}{\partial r}(rE_\theta) &= -i\omega B_z \\ ik_z B_\theta &= i\frac{\omega}{c^2}K_\perp E_r - K_\times E_\theta \\ ik_z B_r - \frac{\partial B_z}{\partial r} &= \frac{i\omega}{c^2}(K_\times E_r + K_\perp E_\theta) \\ \frac{1}{r}\frac{\partial}{\partial r} r B_\theta &= \frac{i\omega}{c^2}K_\parallel E_z. \end{aligned} \quad (5)$$

We then arrive at

$$K_\perp \frac{1}{r}\frac{\partial}{\partial r}\left(r\frac{\partial E_z}{\partial r}\right) + K_\parallel(k_0^2 K_\perp - k_z^2)E_z = \omega k_z K_\times B_z.$$

Using B_θ for boundary conditions we find

$$\begin{aligned} E_z^{(i)} &= H_0^{(1)}(p_i r) \\ H_z &= \alpha\frac{c - p_1^2}{\mathcal{D}}E_z^{(1)} + \beta\frac{c - p_2^2}{\mathcal{D}}E_z^{(2)}, \end{aligned} \quad (6)$$

where $H_0^{(1)}$ is the *Hankel function of zeroth kind*, and we can solve for α and β by setting boundary conditions on E_z and B_θ at the antenna.

3.2 Application to a small dipole

We then consider a small dipole, where we have

$$\begin{aligned} I &= I_0 \sin\beta(|z| - L) \\ V &= V_0 \cos\beta(|z| - L) \end{aligned} \quad (7)$$

and we apply the Fourier transform with respect to z to get I_s and V_s.

Matching H_θ at an antenna of radius r_0 allows us to get

$$\begin{aligned} E_z(r_0) &= \alpha H_0^{(1)}(p_1 r_0) + \beta H_0^{(1)}(p_2 r_0) \\ E_z'(r_0) &= \alpha p_1 H_0^{(1)'}(p_1 r_0) + \beta p_2 H_0^{(1)'}(p_2 r_0) \\ B_z(r_0) &= \alpha\frac{c - p_1^2}{\mathcal{D}}H_0^{(1)}(p_1 r_0) + \beta\frac{c - p_2^2}{\mathcal{D}}H_0^{(1)}(p_2 r_0) \end{aligned} \quad (8)$$

Now we can set up the following system:

$$\begin{pmatrix} H_0^{(1)}(p_1 r_0) & H_0^{(1)}(p_1 r_0) \\ A_{21} & A_{22} \end{pmatrix} \begin{pmatrix} \alpha \\ \beta \end{pmatrix} = \begin{pmatrix} ik_z V_s \\ \frac{i\omega\mu_0}{k_0^2 2\pi r_0} I_s, \end{pmatrix} \tag{9}$$

$$A_{21} = \frac{K_\perp(k_0^2 K_\perp - k_z^2) + k_0^2 K_\times^2}{D} p_1 H_0^{(1)}(p_1 r_0) + \omega k_z \frac{K_\times}{D} \frac{c - p_1^2}{\mathcal{D}} p_1 H_0^{(1)}(p_1 r_0)$$

$$A_{22} = \frac{K_\perp(k_0^2 K_\perp - k_z^2) + k_0^2 K_\times^2}{D} p_2 H_0^{(1)}(p_2 r_0) + \omega k_z \frac{K_\times}{D} \frac{c - p_2^2}{\mathcal{D}} p_2 H_0^{(1)}(p_2 r_0). \tag{10}$$

Finally, the electric field E_z(r) will be given by:

$$\int_{-\infty}^{\infty} e^{-ik_z z} \frac{H_0^{(1)}(p_1 r)\left(A_{22} ik_z V_s - A_{12}\frac{i\omega\mu_0 I_s}{2\pi r_0 k_0^2}\right)}{A_{11}A_{22} - A_{12}A_{21}}\, dk_z + \int_{-\infty}^{\infty} e^{-ik_z z} \frac{H_0^{(1)}(p_2 r)\left(A_{11}\frac{i\omega\mu_0 I_s}{2\pi r_0 k_0^2} - A_{21} ik_z V_s\right)}{A_{11}A_{22} - A_{12}A_{21}}\, dk_z, \tag{11}$$

and the magnetic field B_z(r) will be given by:

$$\int_{-\infty}^{\infty} e^{-ik_z z}\left(\alpha \frac{c - p_1^2}{\mathcal{D}} H_0^{(1)}(p_1 r_0) + \beta \frac{c - p_2^2}{\mathcal{D}} H_0^{(1)}(p_2 r_0)\right)\, dk_z. \tag{12}$$

Similarly, we can calculate the other components of the fields, E_r, E_θ, B_r, B_θ, using the formulas for E_z' and B_z':

$$\begin{aligned}
E_z' &= \alpha p_1 H_0^{(1)'}(p_1 r) + \beta p_2 H_0^{(1)'}(p_2 r) \\
B_z' &= \alpha p_1 \frac{C - p_1^2}{\mathcal{D}} H_0^{(1)'}(p_1 r) + \beta p_2 \frac{C - p_2^2}{\mathcal{D}} H_0^{(1)'}(p_2 r) \\
E_\theta &= \int_{-\infty}^{\infty} e^{-ik_z z}\left(\frac{-ik_z k_0^2 K_\times}{D} E_z' + \frac{i\omega(k0^2 K_\perp - k_z^2)}{D} B_z'\right) dk_z, \\
E_r &= \int_{-\infty}^{\infty} e^{-ik_z z}\left(\frac{ik_z(k_0^2 K_\perp - k_z^2)}{D} E_z' + \frac{i\omega(k0^2 K_x)}{D} B_z'\right) dk_z, \\
B_\theta &= \int_{-\infty}^{\infty} e^{-ik_z z}\left(-\frac{i}{\omega}\left(\frac{k_0^4 K_\perp^2 - k_0^2 k_z^2 K_\perp + k_0^4 K_\times^2}{D}\right) E_z' - ik_z \frac{k0^2 K_\times}{D} B_z'\right) dk_z. \\
B_r &= \int_{-\infty}^{\infty} e^{-ik_z z}\left(\frac{-ik_z^2 k_0^2 K_\times}{\omega D} E_z' + \frac{ik_z(k0^2 K_\perp - k_z^2)}{D} B_z'\right) dk_z,
\end{aligned} \tag{14}$$

All fields are scaled by $\frac{1}{2\pi}$.

3.3 Varying the angle θ between the antenna and B_0

In the case where we vary the angle θ between the antenna and the direction of the magnetic field B_0, using the dielectric tensor adds another level of complexity to the Maxwell equations to be solved.

In that case the equations to be solved are:

$$\begin{aligned}
-ik_z E_\theta &= -i\omega B_r \\
ik_z E_r - \frac{\partial E_z}{\partial r} &= -i\omega B_\theta \\
\frac{1}{r}\frac{\partial}{\partial r}(rE_\theta) &= -i\omega B_z \\
ik_z B_\theta &= aE_r + bE_\theta + cE_z \\
ik_z B_r - \frac{\partial B_z}{\partial r} &= dE_r + eE_\theta \\
\frac{1}{r}\frac{\partial}{\partial r} rB_\theta &= fE_r + gE_z,
\end{aligned} \tag{15}$$

where $a = \frac{i\omega}{c^2}K_\perp - k_z^2\cos^2\theta$, $b = \frac{i\omega}{c^2} - K_\times$, $c = \frac{i\omega}{c^2}k_z^2\cos\theta\sin\theta$, $d = \frac{i\omega}{c^2}K_\times$, $e = \frac{i\omega}{c^2}K_\perp - k_z^2$, $f = \frac{i\omega}{c^2}k_z^2\cos\theta\sin\theta$, $g = \frac{i\omega}{c^2}K_\parallel - k_z^2\sin\theta$.

We then have

$$\begin{aligned}
\frac{\partial E_z}{\partial r} &= i\omega B_\theta + \frac{k_z^2}{a}B_\theta - \frac{ibk_z}{a}E_\theta - \frac{ik_z c}{a}E_z \\
\frac{\partial B_z}{\partial r} &= \frac{idk_z}{a}B_\theta + \frac{bd}{a}E_\theta + \frac{cd}{a}E_z - eE_\theta + \frac{ik_z^2}{\omega}E_\theta
\end{aligned}$$

$$E_\theta = E_z\left(\frac{-c}{b} - ct_1\left(\frac{bd}{a} + \frac{ct_2 ik_z c}{a}\right)\right) - \frac{\partial E_z}{\partial r}\left(\frac{a}{ibk_z} + ct_1 ct_2\right) + ct_1\frac{\partial B_z}{\partial r}$$

$$B_\theta = \frac{\partial B_z}{\partial r}\frac{1}{1 - ct_2(i\omega + kz^2/a)} - E_z\frac{\frac{cd}{a}\frac{ct_1 ik_z c}{a}}{1 - ct_2(i\omega + kz^2/a)} - ct_2\frac{\partial E_z}{\partial r}, \tag{13}$$

where $ct_1 = \frac{a}{ibk_z}(i\omega + k_z^2/a)(\frac{1}{1 - ct_2(i\omega + k_z^2/a)})$ and $ct_2 = (\frac{c}{b} - \frac{bd}{a} - \frac{ik_z^2}{\omega})\frac{a}{ibk_z}$.

4 Radiation patterns

A *radiation pattern* shows the relative far field strength of the quantity considered versus angular direction at a fixed distance from the antenna. Since we are dealing with a dipole antenna, the *azimuth plane pattern* is formed by slicing through a 3D pattern in the horizontal plane, the $x-y$ plane in this case, while the *elevation/polar plane pattern* is formed by slicing the 3D pattern through an orthogonal plane (either $x-z$ or $y-z$). One quantity we are especially interested in is the Poynting vector, which is defined as $\mathcal{S}_{ave} = \frac{1}{2}Re(E \times H^*) = \frac{1}{2}Re(E_\phi H_\theta^* - E_\theta H_\phi^*)$. A plot of the time-averaged, Poynting vector, $|\mathcal{S}_{ave}|$ for a fixed distance r is also called the power pattern of the antenna, and it is important as it describes the total power radiated by an antenna.

Here we show characteristic radiation patterns for **various phase velocities** for the Poynting vector and each component of the Electric and Magnetic fields.

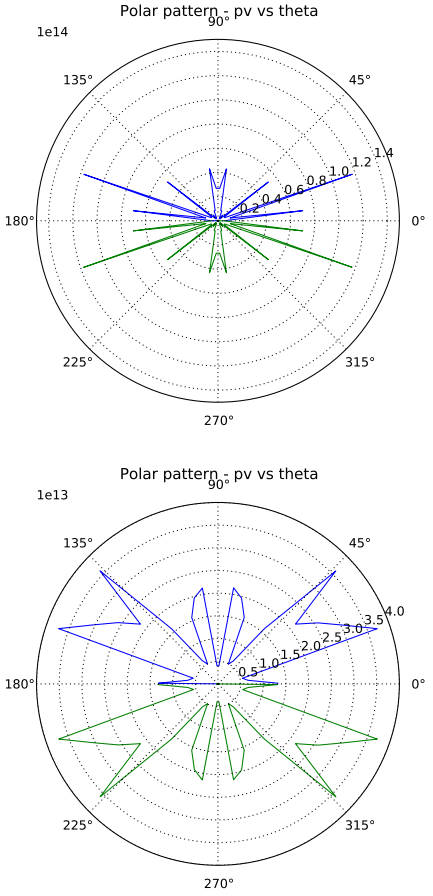

.

Figure 1: Polar Patterns for **S**, $rsph = 200$ and $rsph = 500$, $L = 100$, $\omega = 10000$

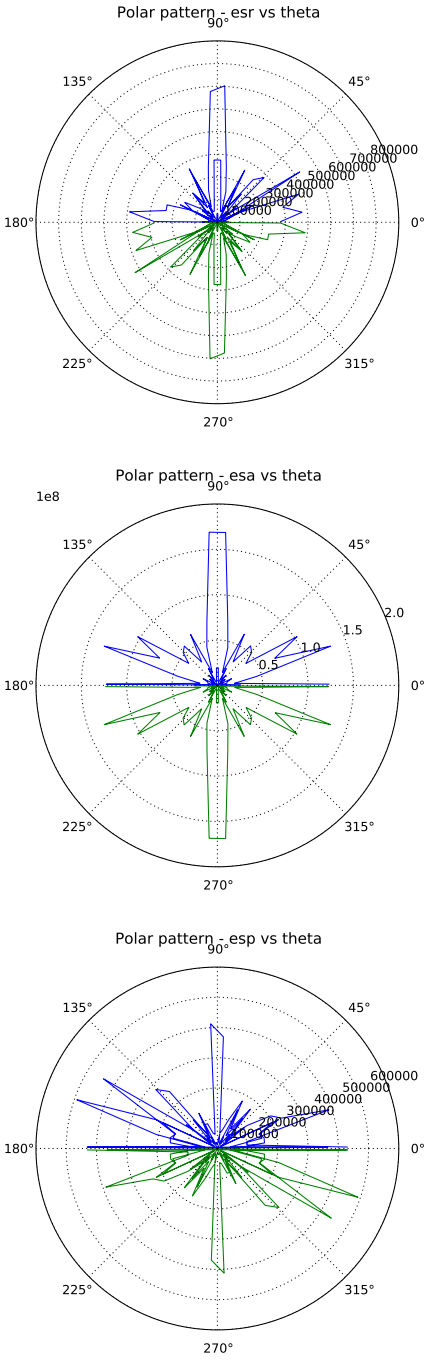

Figure 2: Polar Patterns for **E**, $rsph = 500$, $L = 200$, $\omega = 10000$

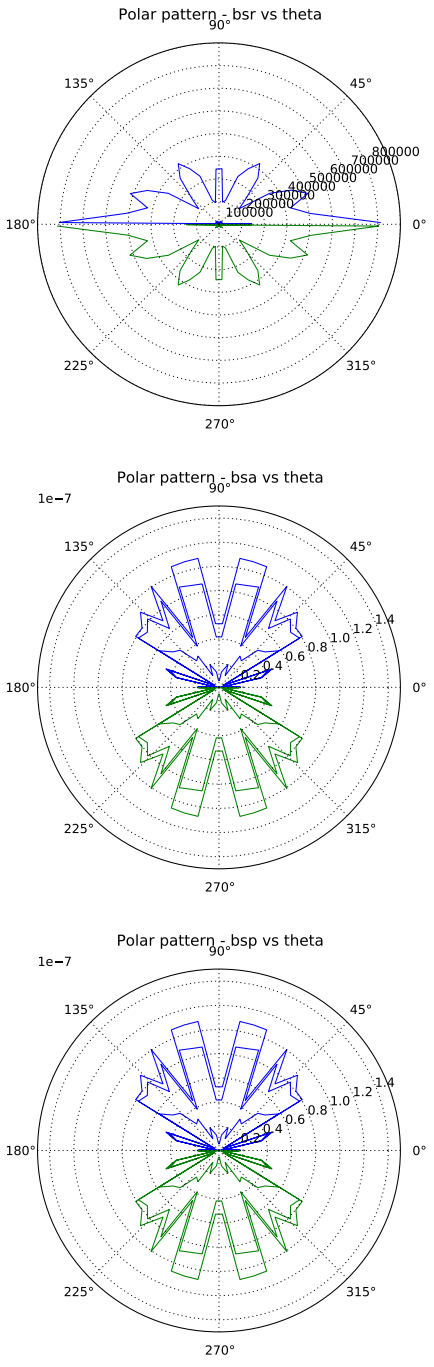

Figure 3: Polar Patterns for **H**, $rsph = 500$, $L = 200$, $\omega = 10000$

5 Analysis

We begin by remarking a few interesting general characteristics that will allow us to draw connections among various types of patterns and parameters. In the VLF range in the magnetosphere, for frequencies higher than the proton gyrofrequency, it is known that in general the only propagating electromagnetic mode is the whistler mode, and consequently only this mode can contribute to the radiation power from a VLF antenna. A main, center lobe due to a principal saddle point implies that almost all the radiation output is contained in that area, and this produces a *focusing effect*. Other lobes result from radiation focusing that is due to the presence of inflection points on the whistler-mode refractive index surface. These *side lobes* can give rise to *nulls* which would correspond to regions in which the antenna does not transmit signal/radiation. Thus, exploring how these depend on the antenna length, frequency, the angle it makes with B_0, and other plasma characteristics gives great insight in antenna design.

A big lobe in the radiation pattern signifies that the antenna radiates energy in one main direction. Focusing effects due to whistler inflection points may also occur for ray directions which are inclined to the static magnetic field line direction. This would imply that the radiation patterns from a given source may possess not only one major lobe along the magnetic field line direction, but also an inclined one at a finite angle.

As described in [WB69], the drop-off in wave energy from the lobe maximum can be rapid and thus the longitudinal focusing of VLF waves can be used as a means of obtaining enhanced wave amplitudes from a low-power satellite transmitter. The fact that some sources may give rise to radiation patterns with not only a major lobe along the magnetic field line direction, but also another which is inclined at some finite angle to this direction, implies that the focusing effects may also occur for ray directions which are inclined to the static magnetic field line direction. Whether or not the longitudinal lobe will predominate in an experimental situation will depend upon the scale of homogeneity of the magnetospheric plasma as well as upon the details of the radiating source.

We will investigate the radiation patterns as the phase velocity vary. We attempt to arrange the radiation plots in such a way to emphasize common characteristics, with varying phase velocities, lengths, radii.

The plots we are going to refer to in our specialized analyses appear below:

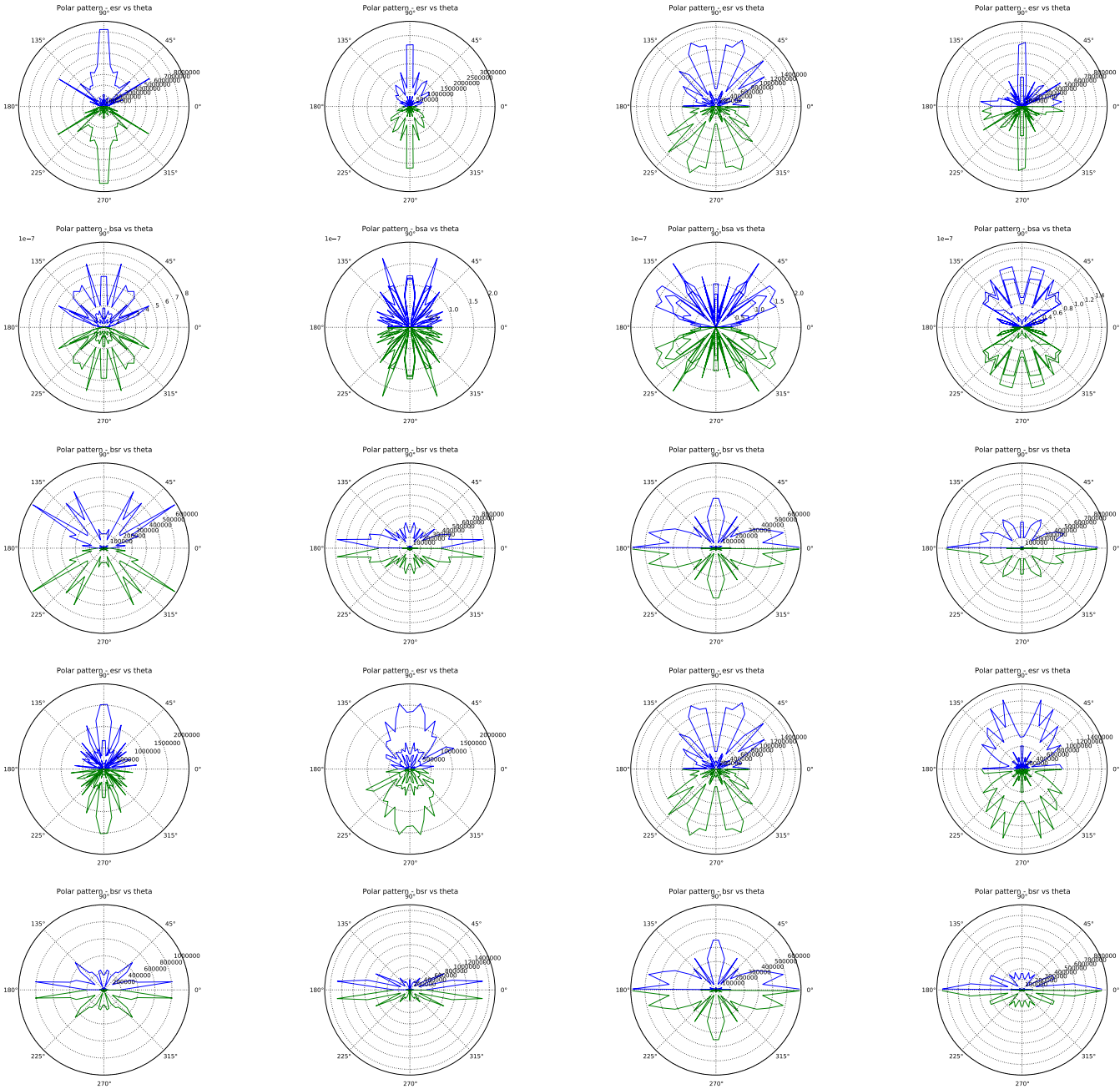

Figure 4: First row: radiation patterns of E_r at a spherical radius of 500, a frequency $\omega = 10000$, and to an antenna of varying lengths: $10, 50, 100, 200$. Second row: radiation patterns of the spherical H_θ at a spherical radius of 500 and a frequency $\omega = 10000$, and to an antenna of varying lengths: $10, 50, 100, 200$. The third row: radiation patterns of H_r at a spherical radius of 500 and a frequency $\omega = 10000$, and to an antenna of varying lengths: $10, 50, 100, 200$. The fourth row: radiation patterns of the E_r of an antenna of length 100, and considered at various spherical radius distances: 200, 300, 500, 1000. The fifth row: radiation patterns of the H_r of an antenna of length 100, and considered at various spherical radius distances: 200, 300, 500, 1000.

In the following sections, we will consider the influence of various factors (phase velocity, antenna length, spherical radius distance, frequency) on the radiation patterns. These considerations will vary in importance depending on the particular application envisioned, for example, for the magnetospheric satellite transmitter described in the introduction. If wave-particle interaction experiments involving particles trapped on field lines that intersect the satellite are of interest, then one needs to maximize the radiation along B_0. However, if an experiment involving wave-propagation is needed, such as in [SA68], then it is important to maximize the radiation at high wave-normal angles, and, particularly, use a parallel electric dipole antenna.

As we will see through these analyses, the far-field behavior of a dipole antenna can be changed by adjusting the plasma frequencies, its length, applied magnetic field, spherical radius distance. The angle that the antenna makes with B_0 also plays an important role, and is the subject of future studies.

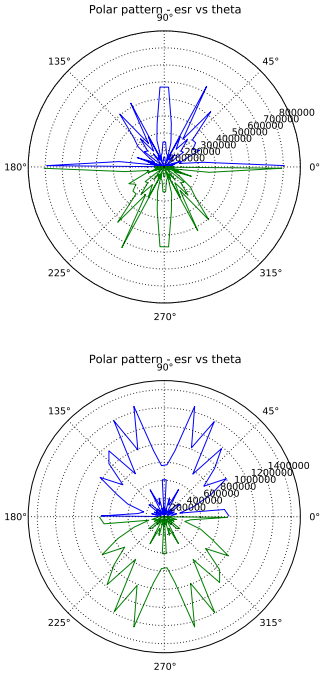

Figure 5: Radiation patterns of E_r at $r_{sph} = 1000$, $L = 200$ and $L = 100$, $\omega = 10000$

5.1 Dependence on the phase velocity

The phase velocity corresponds to the ratio $\frac{\omega_{pe}}{\omega_{ce}}$: the electron gyrofrequency versus the electron plasma frequency. In other words, this quantity measures the angular frequency of the circular motion of an electron in the plan perpendicular to the magnetic field versus the frequency with which electrons oscillate. [ABB] details the regimes corresponding to various phase velocities.

As observed in the plot above, the radiation pattern lobes vary significantly with increasing phase velocities. The power decreases with increasing the collision frequency ω_{ce}. A possible physical explanation for this fact would be that for infrequent collisions, the particles spiral out to large gyroradii where they fall through a large potential difference, therefore absorb more energy from the wave.

5.2 Dependence on antenna length

In a non-plasma medium, the radiation patterns get more interesting as the electrical length of the dipole antennas increase, as more side lobes appear for $L > \lambda$.

The plots corresponding to a varying antenna length are presented in the first and second rows for the spherical radial coordinate of the electric coordinate of the electric field and the elevation coordinate of the magnetic field for the following parameters: spherical radius distance r_sph 500, ω 10000, and lengths varying between 10 and 200.

From the plots, we notice that as L increases, the side lobes of the spherical coordinates of the electromagnetic waves smoothen out and enlarge, while the main lobe expands. This would imply that radiation is focused, and that the nulls of the antenna will enlarge.

On the other hand, the lobes of the Poynting vector will expand as the length of the antenna increases. This would imply that a longer antenna is capable of emitting more radiation across a wider range of directions, which would reduce the size of the nulls.

5.3 Spherical radial magnetic field, Bsr

As noticed in the radiation patterns in the third row in Figure5, the characteristics of the patterns are peculiar for Bsr, as we notice that as L increases, the lobes ply to the sides.

5.4 Dependence on frequencies

We notice the relative distribution of radiated energy is substantially independent of the frequency ω.

As representative radiation pattern plots corresponding to a varying frequency for a dipole antenna we presented below the dependence of the spherical radial coordinate of the magnetic field for the following situations: $r_{sph} = 1000$, $L = 100$, $\omega = 5000$ and $\omega = 10000$.

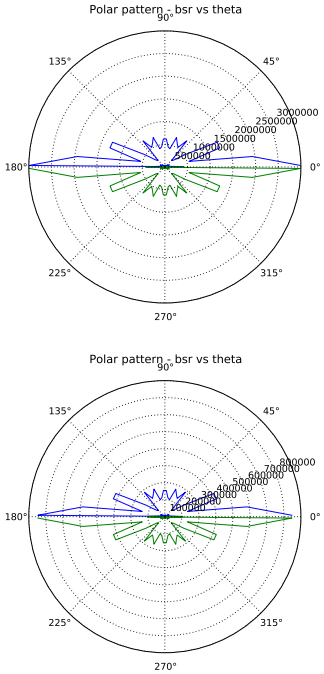

5.5 Dependence on the radius at which the field intensities are considered

The plots corresponding to a varying antenna length are presented in rows four and five of Figure 5. They correspond to the spherical radial coordinates of the electric and magnetic fields for an antenna of length $L = 100$, $\omega = 10000$ and various distances between 200 and 1000.

As the spherical radius distance at which the patterns are considered increases, we notice the lobes shrink and ply to the sides. This would imply that, as expected, radiation varies inversely proportionally with the spherical radius distance, and that the space between the lobes will increase, which means that the antenna nulls will enlarge, causing a loss of radiation/signal.

6 Conclusion

In this paper we have analyzed the problem of electromagnetic radiation from sources in a cold magnetoplasma through the use of cylindrical coordinates in Fourier domain. In applying the resultant formulation, we have considered a small antenna dipole oriented at various angles with respect to the magnetic field. Assuming plasma parameters appropriate to the VLF range in the magnetosphere, we have obtained expressions for the electromagnetic waves and used these to compute the radiation patterns. We have then explored these through varying phase velocities, and considered their dependence on the antenna length, frequencies (ω, ω_{ce}), the angle that the antenna makes with B_0, the radius at which we are obtaining the radiation patterns. We have found that the lobes characteristics and predominance vary substantially with increasing phase velocities, and they either expand or shrink depending on the type of electromagnetic radiation pattern considered. Moreover, we have found that the distribution of the lobes depends on the antenna length, as expected in vacuum. In conclusion, our results show that radiation pattern reshaping is possible by varying the constitutive parameters or operating frequencies for the cold magnetized plasma.

7 Acknowledgments

I thank Pat Colestock and Mark Galassi of Los Alamos National Laboratory for discussions on the problem and software help.

References

[CIS] *Antenna Patterns and their Meaning*, available at `http://www.cisco.com/en/US/prod/collateral/wireless/ps7183/ps469/prod_white_paper0900aecd806a1a3e.html`

[ABB] Allis, W., Buchsbaum S., Bers A. *Waves in Anisotropic Plasmas* (MIT Press, 1963, Cambridge).

[CHE] Chew, W.C. *Waves and Fields in Inhomogeneous Media*, (IEEE PRESS Series on Electromagnetic Waves, 1999).

[OHN94] Ohnuma, T. *Radiation phenomena in Plasmas* (World Scientific Publishing, 1994, Singapore).

[WB69] T.N.C Wang and T.F. Bell. *On VLF Radiation Fields along the static magnetic field from sourced immersed in a magnetoplasma. (IEEE Transactions on Antennas and Propagation, November 1969.*

[WB72] T.N.C Wang and T.F. Bell. *VLF/ELF Radiation patterns of arbitrarily oriented electric and magnetic dipoles in a cold lossless multicomponent magnetoplasma* Journal of Geophysical Research, vol 77, no. 7, 1972.

[WW93] Y. Wenyan and W. Wenbing. *Radiation characteristics of dipole antenna in a grounded composite magnetized semiconductor plasma.* International Journal of Infrared and Millimeter Waves, Vol. 15, No. 2, 1994.

[WB692] T.N.C Wang and T.F. Bell. *On VLF radiation fields along the static magnetic field from sources immersed in a magnetoplasma.* IEEE Transactions on Antennas and propagation, Nov. 1969.

[SHM] E. Soliman, A. Helaly, A. Megahed. *Propagation of electromagnetic waves in planar bounded plasma region.* Progress in Electromagnetics Research, Vol. 67, pp. 25-37, 2007.

[SA68] R.L. Smith and J.J. Angerami, Magnetospheric properties deduced from Ogo 1 observations of ducted and nonducted whistlers, *J. Geophys. Res.*, 1-20, 1968.